Non-linear Internal Loads Modeling Methods

Frank A. Smith Jr.
frank.a.smith2@boeing.com

Paul M. Hopkins
paul.m.hopkins@boeing.com

The Boeing Company, Integrated Defense and Space Systems, Rotorcraft – Philadelphia, PA

Abstract: The current practice at Boeing rotorcraft for determining the distribution of internal forces in aircraft, involves building a finite element model of the aircraft, and applying rotor hub loads, balanced with inertia relief loading to emulate the various mass and maneuver configurations which can occur. These load cases are then solved with a linear static analysis, using NASTRAN© CSHEAR elements to account for buckling of thin shells. Over the past 8 years, efforts have been made to change these assumptions by using a high density mesh on the model, and solving the models with a non-linear analysis in ABAQUS©. The intent is that a more accurate understanding of the actual load paths in the vehicle will result in more uniform actual margins of safety, and thus lead to a more reliable and durable aircraft. Data has been collected from various research projects and production implementations of this technology which indicate that the time for such an analytical approach is near.

This research was partially funded by the Aviation Applied Technology Directorate under Technology Investment Agreement No. DAAH 10-02-2-000 1. The U.S. Government is authorized to reproduce and distribute reprints for Government purposes notwithstanding any copyright notation thereon.

The views and conclusions contained in this document are those of the authors and should not be interpreted as representing the official policies, either expressed or implied, of the Aviation Applied Technology Directorate or the **U.S.** Government.

1. Introduction

The use of NASTRAN© CSHEAR elements is a widely spread practice in the rotorcraft industry for modeling thin webs and skins which are likely to buckle under ultimate loads. These elements possess only shear stiffness, in an attempt to account for the loss of bending and extensional stiffness which happens when the web bay fully buckles. This assumption is made in an attempt to avoid having to mesh the model finely, and run it non-linearly, both of which substantially add to the runtime of the analysis. Although it is possible to run such models, the challenge is in running several hundred load cases in a timely manner. This includes both pure central processing unit (CPU) time, and engineering time to submit and monitor jobs, and ensure that a converged answer is obtained. In the last 8 years, work has been done at Boeing to develop non-linear detailed finite element analysis (FEA) skills using ABAQUS© to remove many of the assumptions made in the current analysis process.

The current process for general aircraft frame sizing uses the internal loads models as just described, run linearly. The internal forces (element forces and freebody summations) are then extracted from the model and margins of safety are then calculated with closed form solutions for stress, stability, and other factors. These margins of safety are used to size the aircraft's structural members.

A new process is being proposed, where the internal loads model will have a mesh fine enough to capture the post-buckled response and load re-distribution. These results will then be used to identify a critical load case for the part, through max/min searches of stresses or strain energy summations. A more detailed model of the part of interest will then be built, and either analyzed integrated into the full loads model, or analyzed using some form of sub-modeling procedure. This new process will lead to a more uniform real margin of safety for the aircraft, and thus provide cost savings on many levels for Boeing and its customers.

2. Earlier Research and Production Implementations

In the late 1990's and early 2000's the focus was on detailed stress analysis with fine meshed models. Most stress analysis at that time was performed by pulling element forces from the crude meshed internal loads models, and then using the in-house software, Integrated Analysis Software (IAS), or Microsoft Excel spreadsheets to automate the process of performing hand calculations for Margins of Safety on stress and stability. The use of detailed meshes to obtain stresses was in use, but not wide spread. As the early 2000's came about, detailed FEA was becoming more accepted and more common, but it was seen that performing non-linear analyses would require much better computing resources than was available to the stress group here. There was a desire to perform post-buckled analysis, as well as contact analyses for assemblies of rotor parts. By the end of 2001 the business case was made and accepted to invest in computing equipment to allow these improvements in our processes.

2.1 Identification of the Magnitude of Stiffness Mismatch

By 2003 the new computing resources were in place, including an IBM p690 with 12 processors and 24 Gb RAM, and a LINUX cluster with 32 dual CPU nodes to handle the new generation of stress analyses. During that year, work was done as part of the Survivable Affordable Repairable Airframe Program (SARAP), to perform global to local modeling on a rotorcraft to show our ability to predict co-cured stiffener de-laminations. A quarter section of the fuselage was modeled in more detail for the purpose of performing a post-buckled analysis on a known test condition which had a co-cured stiffener de-lamination at a known load level.

The internal loads model was run with the desired load case, and then those results had to be somehow mapped onto the new fine meshed section. There are 2 basic methods of doing this, mapping displacements, or applying forces from the loads model. First, displacement mapping was attempted, where the displacements of the internal loads model are applied to the boundaries of the detailed model. This has the merit of making it easy to apply the boundary conditions, since they are directly taken from the model. The results of this method showed stresses much higher than anticipated. When the second method, applying forces from the loads model, was attempted, the displacements in the model were generally too high. The displaced shape was also globally wrong, without appropriate boundary conditions to restrain it. Strain energy for the whole model also was lower in the detailed model with applied forces, indicating either missing forces, or lower stiffness (due to lack of adequate boundary restraint)

In order to understand why this was happening, a comparison of the stiffness of the two fuselage section models was made. Two models were examined, the first one being the detailed fuselage section, and the second being the comparable section from the loads model. The forward end was fixed, and the aft end had a rigid MPC attached from all the end nodes to one control node. This control node then had a displacement applied to it. The original internal loads model was run with a linear static analysis, and the detailed section was run with a non-linear static analysis. The stiffness was calculated as the sum of the reaction forces at the held side divided by the applied displacement at the other side. Global strain was calculated as the applied displacement divided by the original length of the fuselage section. Figure 1 illustrates the trend of the data comparing non-linear detailed FEA vs. CSHEAR and bar type modeling.

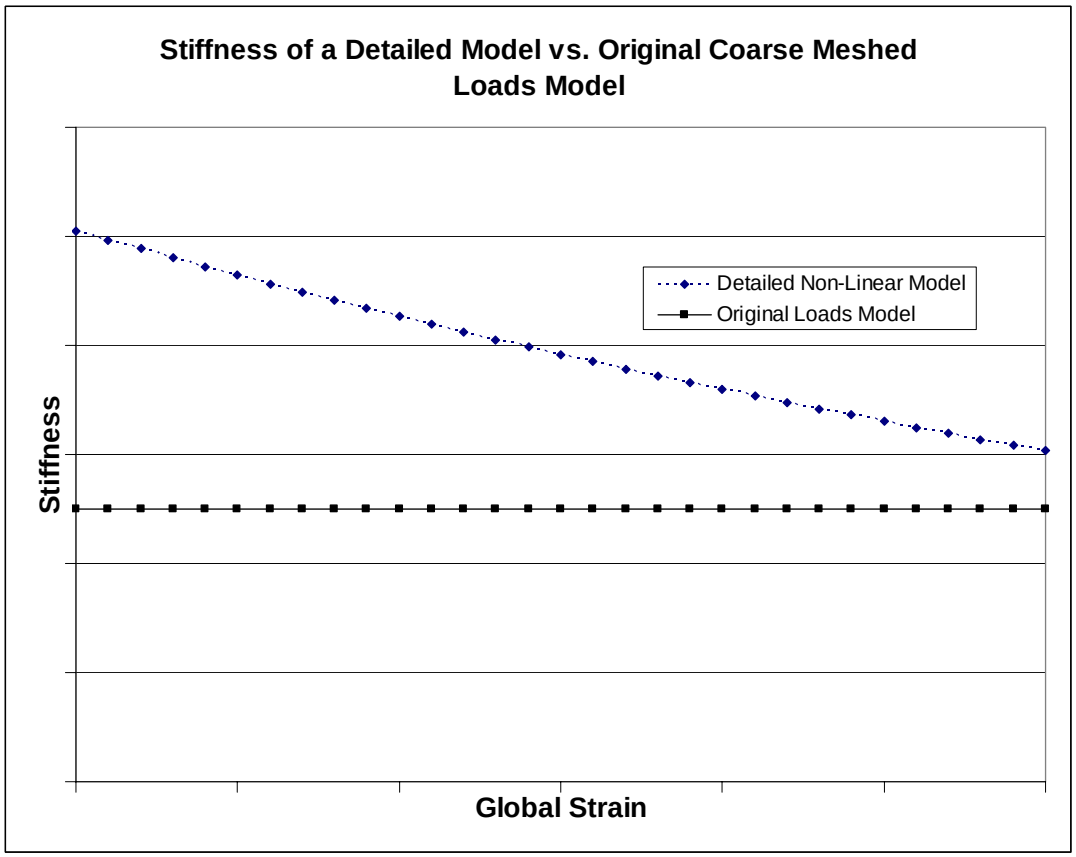

Figure 1 –Stiffness of a non-linear detailed model and current internal loads model of a section of rotorcraft fuselage

As can be seen in Figure 1, there is a large difference in stiffness between the internal loads model and the detailed model of the section of fuselage at low strain levels. As global strain increases, the non-linear model's stiffness approaches that of the internal loads model. This is caused by the use of NASTRAN© CSHEAR elements to model the skin and attempt to account for post-buckled stiffness changes. In the non-linear model, the skin carries significant extensional load, until the thin panels buckle, and then as the load increases it approaches the assumption that post-buckled panels carry little extensional load, but maintain shear stiffness. It can be seen from the graph above, that at ultimate load levels, the CSHEAR assumption nears reality, but at lower load levels, such as in fatigue conditions, there is considerable divergence.

The philosophy illustrated here is that current modeling methods provide generally conservative loads for the airframe which can be obtained quickly, since the models are analyzed linearly. Several problems are also implied, though. In a flight condition where the aircraft fuselage can be visualized as a beam, the bending produces compression on one side and tension on the other. Therefore the stiffness on the tension side of the fuselage will globally be too compliant by 100% or so at all load cases. Also, with such a non-uniform difference between actual stiffness (assuming that the non-linear model better reflects reality) and modeled, the true effect on the load path is not clear, and thus it can't be assured that the load distribution will always be conservative.

Historically, generally minor structural problems are seen in these aircraft when testing or in flight when observing its ability to reach limit or ultimate loads. This would indicate that the current method is adequate to design a safe aircraft, at least when used in conjunction with test. The more significant issues arise in fatigue testing or long service time, where the load levels of interest are lower, and thus the internal loads predictions are less accurate since the stiffness is further away from reality. This would indicate that it should be possible to improve the aircraft's durability by these newer methods.

2.2 Early Production Implementation of New Modeling Methods - CH-46E

The United States Navy currently makes use of a fleet of CH-46 helicopters, and has since the first CH-46A was completed for the Marines in 1962. During the 1980's the existing CH-46 fleet was upgraded to the CH-46E configuration, which included a larger stub-wing to accommodate a larger fuel tank (see Figure 2). The stub-wing houses the main landing gear as well as the fuel tank and other equipment. Since this upgrade to the CH-46E, it was noticed that the new models exhibited fatigue cracking at the attachment locations for the stub-wings.

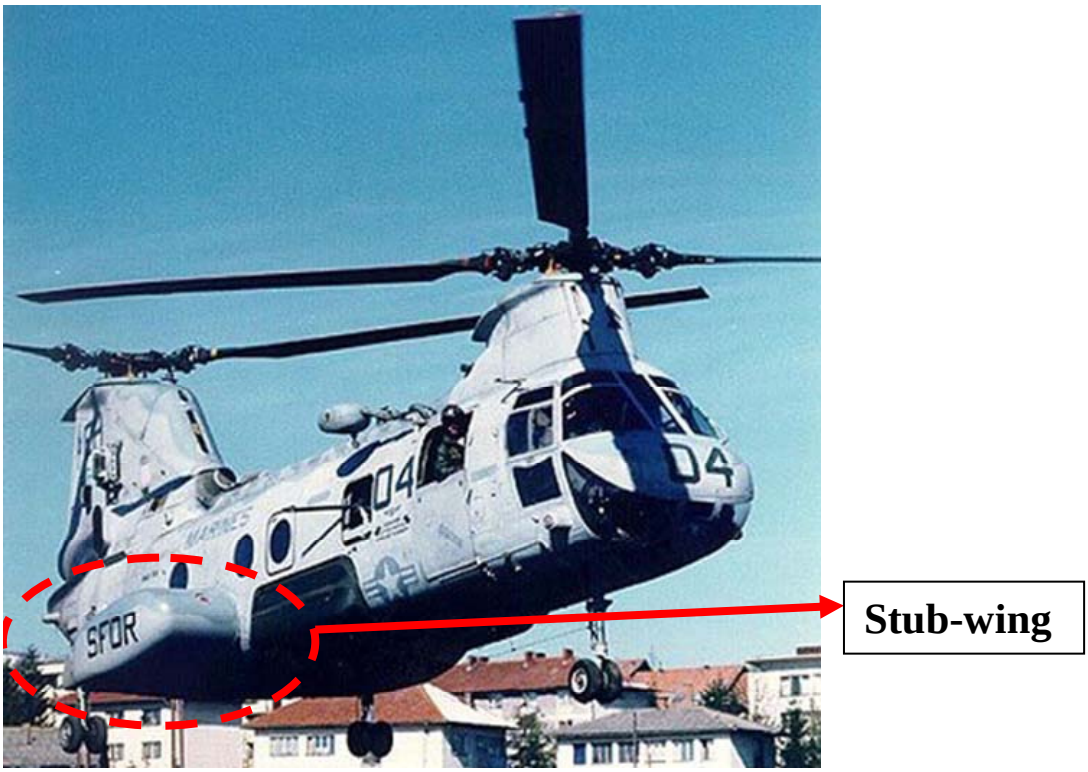

Figure 2 – CH-46E helicopter, showing location of stub-wing

This cracking occurs in the stub-wing fittings as well as the airframe close to the attachment locations. In 2003, the Navy requested an engineering investigation into the cause of the cracking.

In support of this investigation, a model of the full aircraft was obtained from the Navy. This model had a crude mesh with typically one element per skin bay height. This original model used a shell and bar modeling scheme. A full fuselage section of the model around the stub-wing was modeled with a 1" mesh. In the areas of interest, near the stub-wing connections, the mesh was refined to ¼", and the stub-wing fittings themselves were modeled with tet10 solids. Frames and longerons were modeled full-depth with shells, and skin stiffeners with beam elements. All shell meshed parts were connected together with beam type MPCs. This refined model (see Figure 3) was run in ABAQUS© for various load cases and mass configurations, with a linear static analysis.

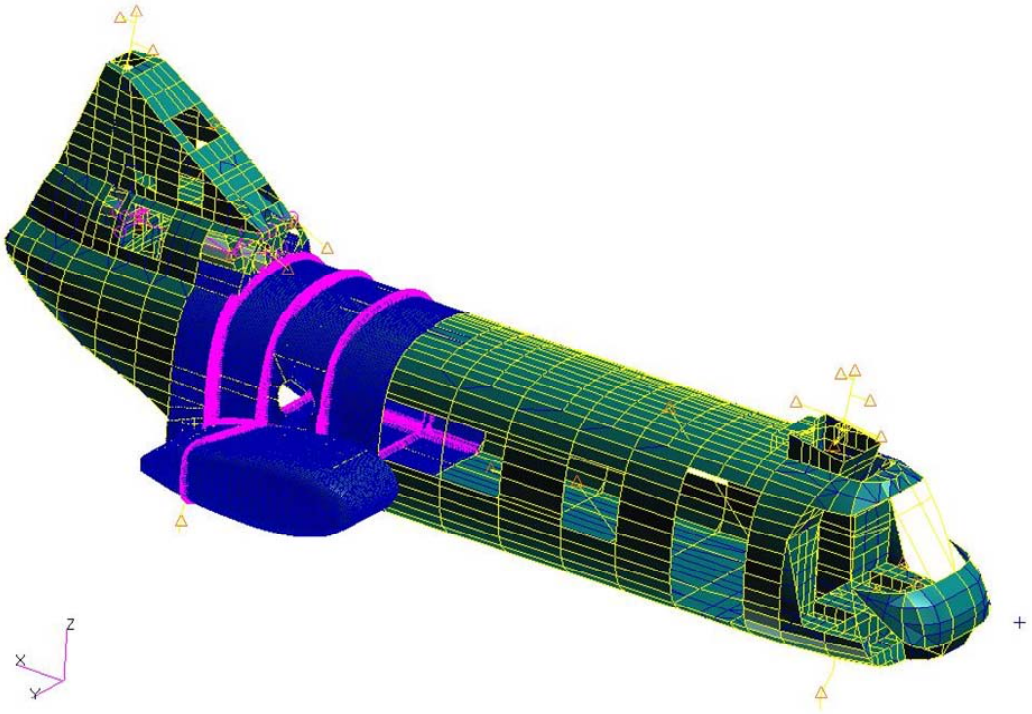

Figure 3 – CH-46E stub-wing attachment investigation model.

The results of this model showed high stresses at the crack locations due to a combination of landing loads and vibratory loads induced by the rotors. Part of this investigation included a verification of the finite element model, using flight test data. For the purpose of furthering the development of non-linear internal loads modeling, this model was run with a non-linear static analysis as well as linear static to see the difference in the results. The finite element models were run with a hover condition, and compared with a level flight condition in test. This could be an obvious source of error in the correlation, but it was considered that the rotor loads should be similar between the two, and level flight hub loads were not available at the time of the correlation. Other sources of error could include mass configuration differences, particularly as fuel was spent during flight, and the fact that fairings were not modeled. It can also be seen that strains (or stresses as plotted) were fairly low for level flight and this makes the test results more susceptible to fluctuations in the gauge data. Even given those factors, correlation to test flight was quite good for most gauges. Each gauge is shown in Figure 4 along with Non-linear and linear FEM predictions. The test data bars represent the average of the means of each peak and valley pair for the selected flight event. The error bars on the test data represent the max and min values of the gauges during the event. The FEA based predictions shown represents the stress at the given location in the model as best as can be determined, and the error bars represent the max and min values of the stress in the elements surrounding the gauge location. Thus the error bars show the variance of the FEM prediction within a ¼” radius of the best estimate of the gauge location.

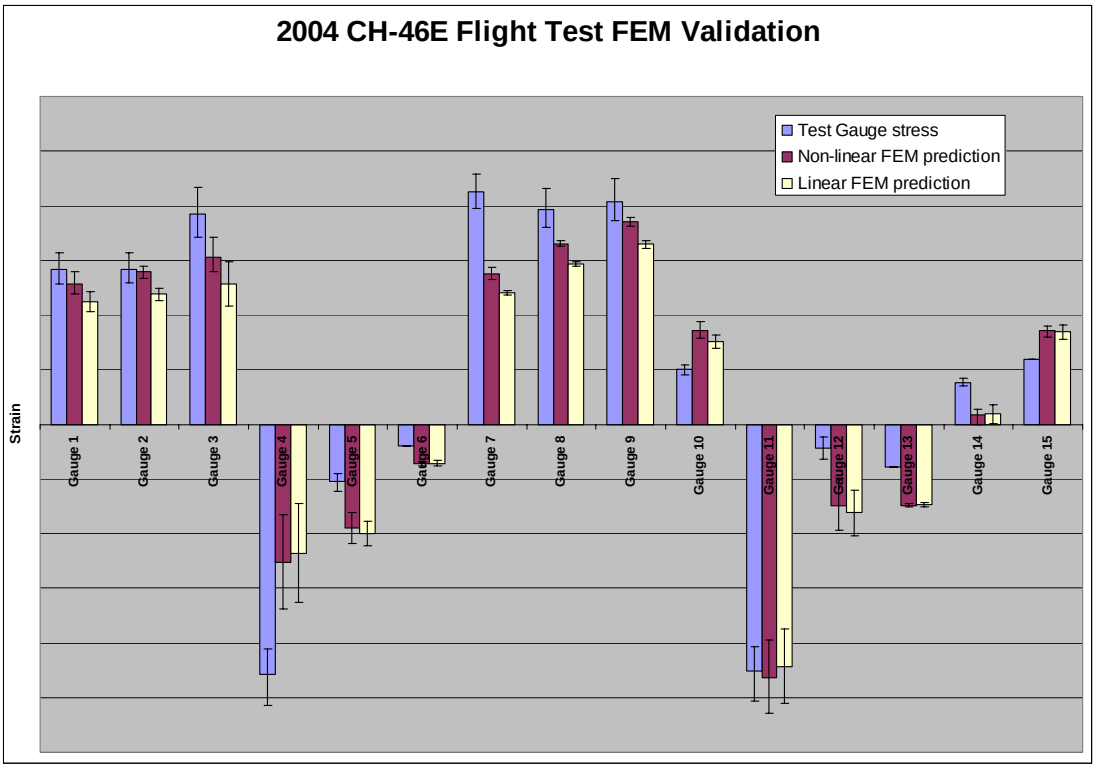

Figure 4 – CH-46E flight test data correlation

Not only are all gauges correctly signed, but the relative magnitudes look about right, and many gauges show overlapping variance bands. It can also be seen that at most gauges, the non-linear results more closely approximate the test results than the linear. Though this data was good, more work may be done in the future to improve this correlation in the ways previously mentioned. Another thing to note is that although a comparison between linear and non-linear results was shown, a comparison between the older CSHEAR modeling method versus the newer non-linear FEM results was not shown. This piece of data is still missing, and would show the true benefit of changing to non-linear internal loads models.

3. Recent Research

3.1 Overview

This year, research was conducted under the Boeing rotorcraft Internal Application Development (IAD) program, to further refine the approach to non-linear internal loads modeling, and answer many questions still remaining on applying this approach to analysis. The process included reviewing the existing common mesh densities used for internal loads models, and determining an acceptable mesh density to capture post-buckling affects shear web panels. Another task was to review solution methods and determine the most efficient one for solving the nonlinear static finite element model (FEM). The last major task was to compare part design procedures and part sizing, using the nonlinear FEA results vs. the linear static results.

3.2 Mesh Density Studies

Following a review of the current mesh densities used for an internal loads model on some common rotorcraft it was determined that the average skin shear panel aspect ratio was approximately 30:6. Using this information, FEM shear web panels were created using a PCL (PATRAN Command Language) based code and solved in ABAQUS©. The models had the same overall dimensions; however the mesh density and the element aspect ratios were changed in order to determine the affects on the post-buckled stiffness. The models were set up as either a 6" x 6" or 6" x 30" planar shell mesh with out-of-plane edge displacements restrained, one corner restrained in the x and y axis directions and one other single node restrained in the y-axis direction to prevent rotation (See Figure 5). The model was analyzed for two separate studies. First, the shear flow was applied to the edge nodes, and an eigenvalue buckling analysis was performed to obtain the lowest critical stress. The second analysis was a two step process, where the first step had a shear flow applied on the edges and run with a non-linear static analysis. In the second step, a small, extensional load was applied and a nonlinear static analysis was performed. The results of the second step were used to determine the extensional stiffness of the panel, by summing the total load applied at the edge and dividing it by the average displacement of the nodes on that edge in the direction of load application. A single, 1lb out-of-plane force was applied at the model center to introduce an imperfection in the geometry and stimulate out-of-plane buckling.

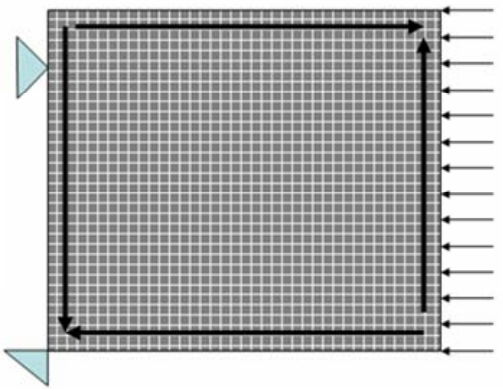

Figure 5 - Shear web FEM for convergence study

Following approximately 500 analyses and completing a mesh convergence study, it was determined that using a ½" element size (12 elements across the small dimension for a 6" x 6" panel) with a 1:1 element aspect ratio was acceptable in capturing the post-buckling stiffness of the web panel. A ¼" element mesh density is preferred; however, due to computer limitations at the present time this is not feasible with respect to time to solve the FEM. Figure 6 shows the post buckled extensional stiffness compared to the element length of a 6"x6" web panel. The convergence of the post-buckled stiffness at and beyond an element length of 0.5" is visually present in this graph.

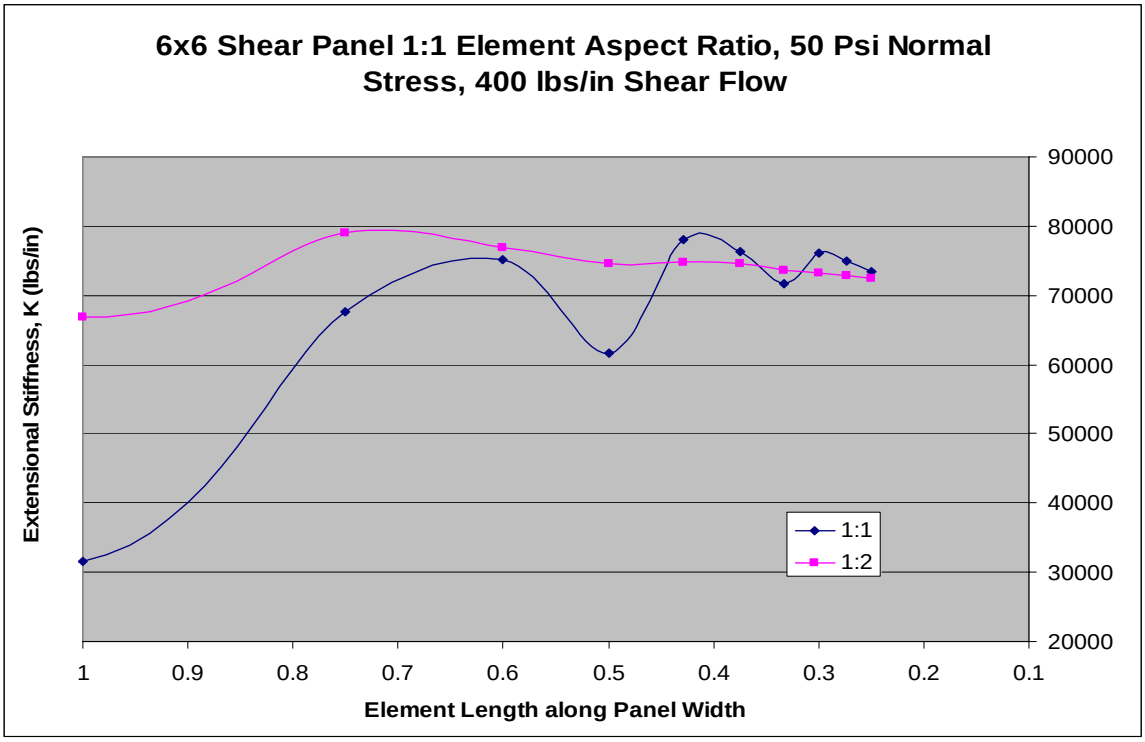

Figure 6 - Extensional stiffness for a 6x6 shear panel, changing with element aspect ratio and element edge length.

Figure 7 shows the critical stress estimated from an eigenvalue buckling analyses for a 6”x30” panel as the element size varies. Different aspect ratios for the elements in the mesh are shown on different curves to illustrate the tolerance to aspect ratio. Also shown on this graph is the critical buckling stress for the panel as predicted by the Boeing Design Manuals (BDMs), which contain empirically derived and/or tested hand calculation methods.

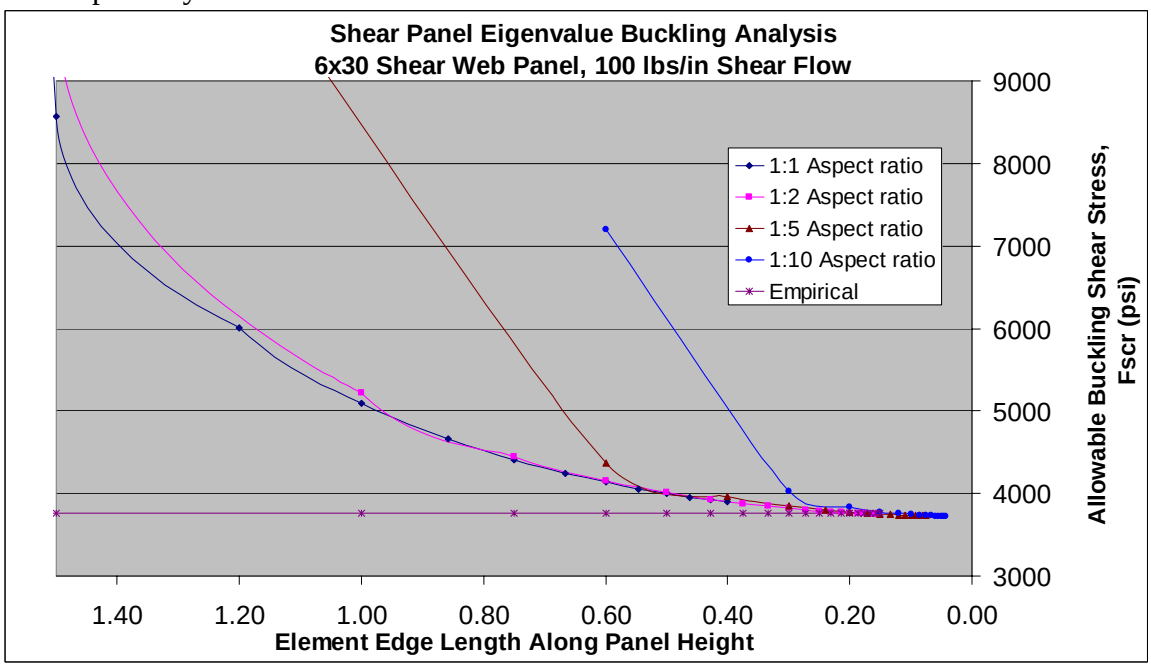

Figure 7 - Critical Shear Buckling Stress Changes with Element Size and Aspect Ratio

It is important to note that a gradual, rather than an instantaneous, drop off in extensional stiffness was shown in the results of the analyses. This is important to present in order to evaluate the process and method of using post-buckling stiffness rather than assuming that under loading, web and skin panels carry shear load only and no extensional load instantaneously after initial buckling. There is however a certain degree of loading that is transferred into the web and skin panels in the form of extensional forces due to the fact that there is extensional stiffness in the post-buckled panel. Figure 8 shows the linear extensional stiffness of a web and the extensional post-buckled stiffness from a non-linear FEM. As the graph shows, there is a drop-off in stiffness of the panel from the linear value towards zero but it is not instantaneous. A CSHEAR element would, of course have an extensional stiffness value of zero over all shear load levels. This graph also illustrates the sensitivity of the solution to initial imperfections. It was found that sometimes, as the load gets well above the critical buckling load, a buckling mode higher than the first mode would sometimes occur. This was prevented by using initial imperfections from an eigenvalue buckling analysis. In Figure 8, it can be seen that when a buckling mode higher than the first is assumed, the extensional post-buckled stiffness is significantly affected. Apparently the nature of the initial imperfection is important, as both of these runs already had a small out-of-plane load applied to stimulate buckling.

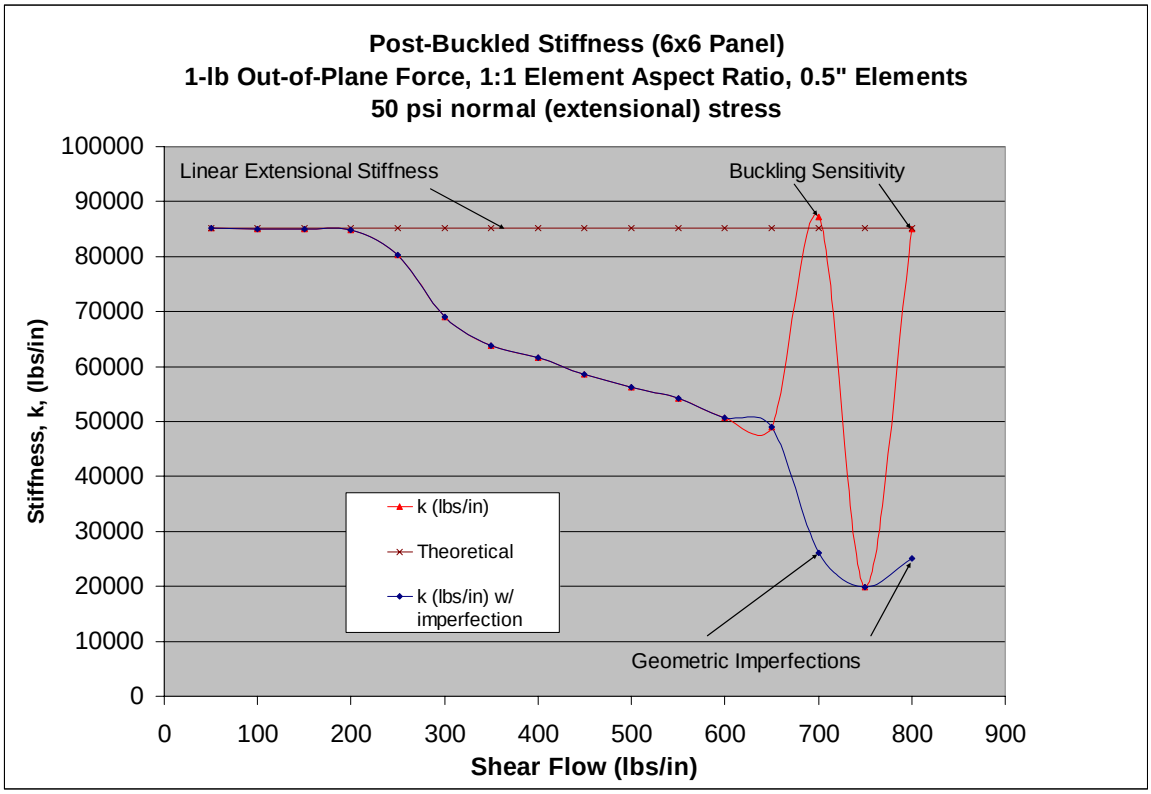

Figure 8 - Post-buckled stiffness 6x6 shear panel with imperfections

3.3 Solution Methods

There were four solution methods investigated in solving the FEA and are listed as follows:

1) Linear Static Analysis
2) Nonlinear Static Analysis with dashpots.
3) Nonlinear Static Analysis with geometric imperfections added from a buckling analysis and inclusion of dashpots.

4) Nonlinear Static Analysis with geometric imperfections added from a linear static analysis and inclusion of dashpots.

The first method is the traditional and simplified linear static analysis. The remaining 3 methods all utilized nonlinear static analysis and dashpots in order to control the instabilities due to the buckling. The second solution used nonlinear static analysis and dashpots alone. The third and fourth solution methods added geometric imperfections to the model in order to expedite the solution process. The third solution method used geometric imperfections from an eigenvalue buckling analysis while the fourth solution method used geometric imperfections from a linear static analysis of the same load case. The four solution methods were compared based on their strain energy, deformations, buckling shapes, modes, and eigenvalues, and most importantly the run time. With the exception of the linear static analysis case, the buckled shapes and magnitudes were all within 1% of each other, therefore the only variable left to compare was the time. Figure 9 and Figure 10 show the comparisons of methods 1 and 2, and methods 3 and 4 respectively, and more specifically, the comparisons of the deformed buckled shapes can be seen. Method 1, the linear static analysis does not present the amount of deformation and thus buckling modes that the other 3 methods do. Furthermore the 3 nonlinear static analysis methods, 2 through 4, have similar, if not almost exact, deformed shapes and magnitudes.

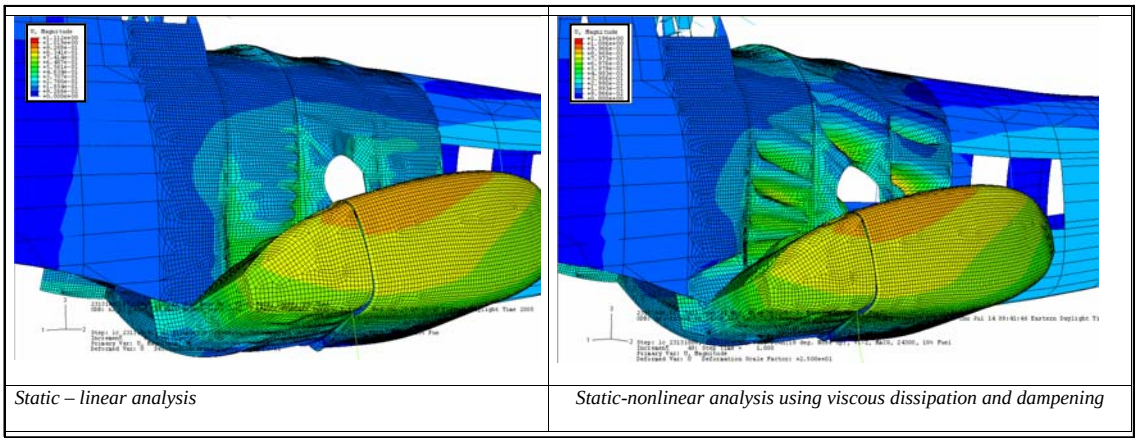

Static – linear analysis	*Static-nonlinear analysis using viscous dissipation and dampening*

Figure 9 - Comparison of linear static analysis and nonlinear static analysis.

In Figure 10, the comparison of the nonlinear static analysis with geometric imperfections from an eigenvalue buckling analysis and a linear static analysis is made and can be seen to be nearly identical in deformed shapes and magnitudes. Once again this iterates that the time to solve the analysis problem will be the major factor in determining the appropriate and efficient solution method.

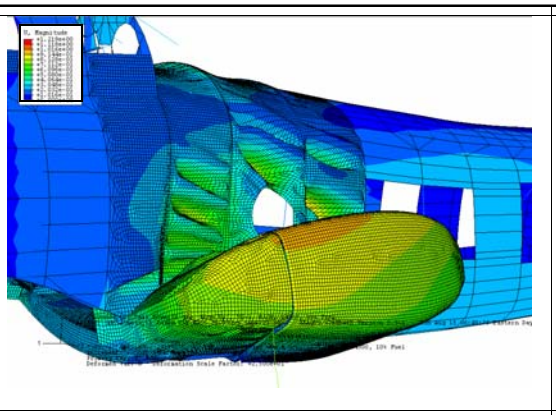

Static-nonlinear analysis using imperfections from a buckling analysis

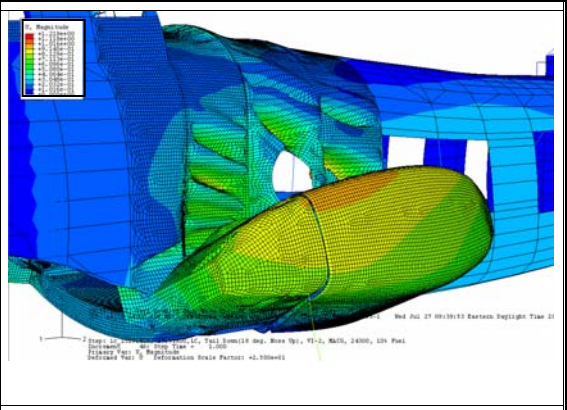

Static-nonlinear analysis using imperfections from a linear static analysis

Figure 10 - Comparison of nonlinear static analyses with geometric imperfections.

Different values of damping coefficients were used for the second solution method and an acceptable damping coefficient of .02 was obtained and incorporated in the third and fourth solution methods. Without the dashpots, the analysis solution failed to converge. Figure 11 shows the CPU time vs. a changing dampening coefficient, and in Figure 12, the viscous damping energy divided by the total strain energy in the model at the end of the solution is plotted vs. the damping coefficient. It can be seen that beyond .02 damping coefficient, there is very little improvement in solution time. Fortunately, the total percentage of energy that goes into damping is still low for all the examined damping coefficients, but since there is little to gain from it after .02, that was the value used.

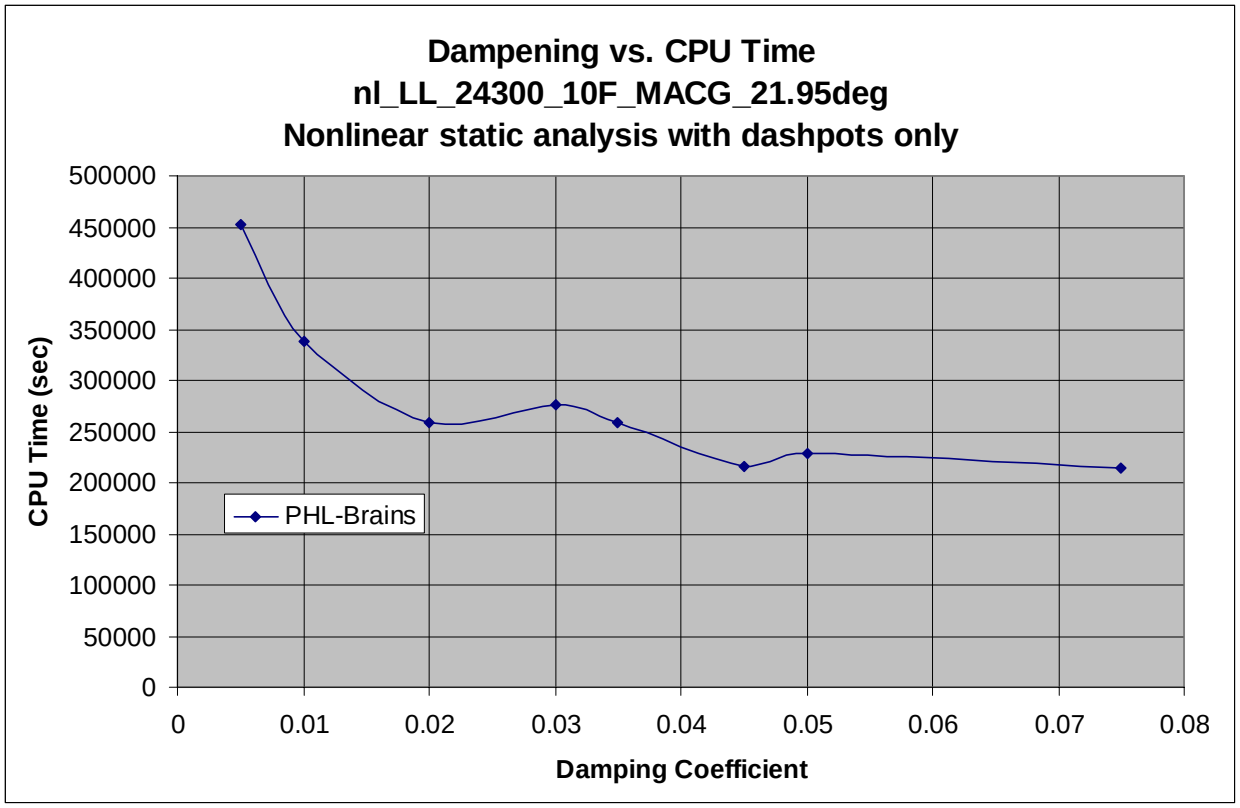

Figure 11 – Solution CPU time vs. damping coefficient

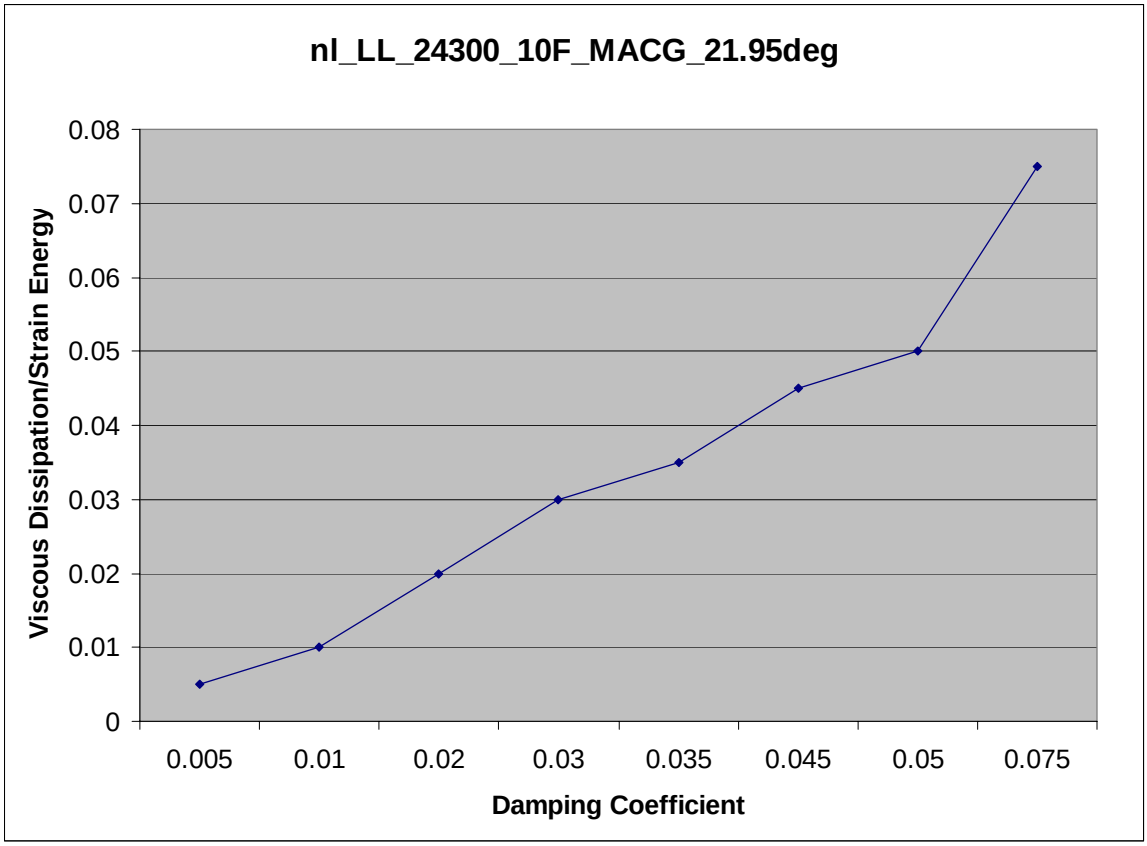

Figure 12 – Percentage of viscous dissipation energy vs. damping coefficient

The imperfection scale factors were then varied in the third and fourth solution method to obtain a set of curves that, theoretically, should have some form of a minima or maxima. The total wall clock time and CPU time was then compared for the 3 nonlinear static analysis solutions and it was determined that adding the geometric imperfections in order to create an expeditious predictive buckling analysis was indeed more time consuming. The eigenvalue buckling or linear static analysis that had to be performed in order to obtain the nodal displacements for the geometric imperfections consumed considerable CPU and Wallclock time such that when compared to the second solution method of using dashpots alone, was not beneficial. Figure 13 shows the total wallclock time of the nonlinear static analyses cases as just described. It is clear from the graph that the inclusion of geometric imperfections adds a considerable amount of run time, approximately 160%, when compared to the use of dashpots alone.

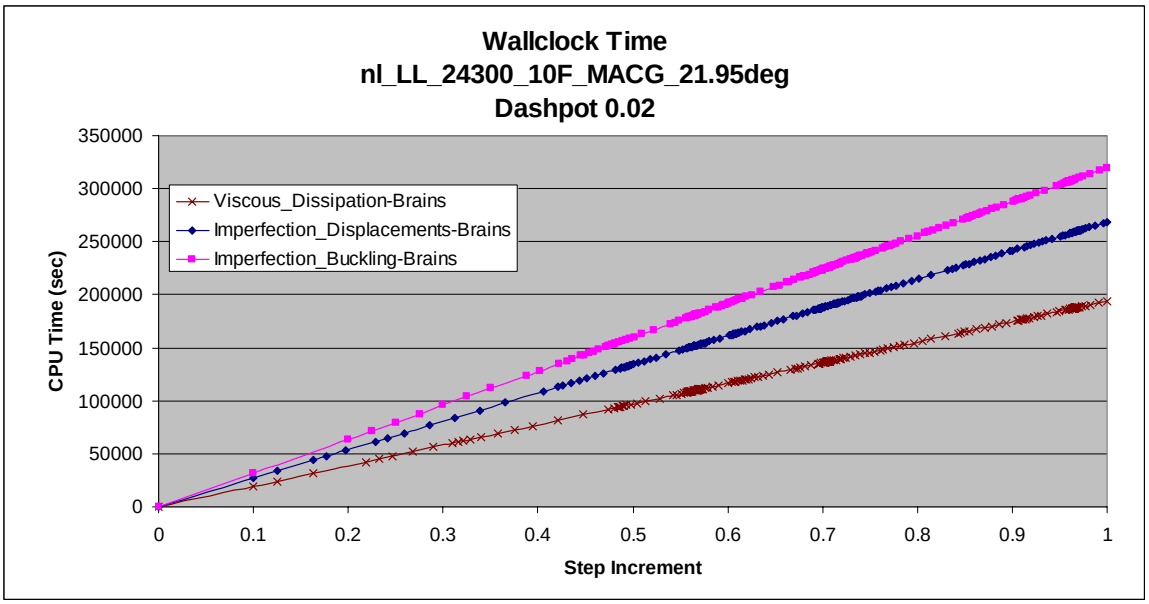

Figure 13 - Total wallclock time for nonlinear static analyses of landing condition.

3.4 Post-processing and Results

At this point the acceptable mesh density has been determined to be ½" for the FEM. The solution method to use is a nonlinear static analysis using dashpots to solve the analysis. There is also knowledge of the fact that the web panels will carry extensional forces rather than shear loading only, and that there still is post-buckled extensional stiffness in the web which will change the load distribution of the structure. This is important to know when sizing the final part for the load in the individual members such as stiffeners, chords and webs where applicable. The situational problem set up here is a fictitious machined part bulkhead with properties and dimensions similar or comparable to an actual rotorcraft bulkhead. The model was set up as a cantilever with a distributed load on top. The bulkhead had bays of 3 rows horizontally and 2 columns vertically as shown in Figure 14.

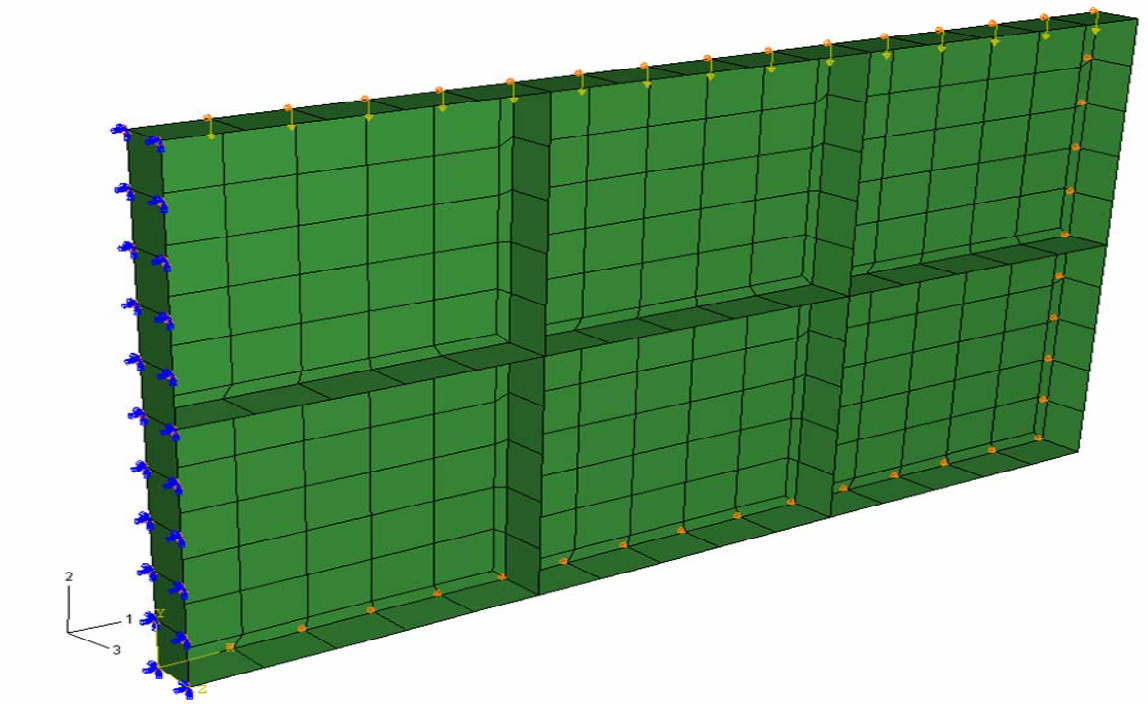

Figure 14 - Machined bulkhead for analysis and design comparisons

There are two major analysis methods to be used on this part which include linear static analysis and nonlinear static analysis. Of these two methods the properties and elements are changed for comparative studies. The following is a list of the analysis methods, the types of elements used, and the post-processing method utilized.

1) Linear static analysis with fully effective quad elements using the Patran© *Results, Create, Free Body* tool. *"Linear Static Analysis Method 1"*
2) Linear static analysis with CSHEAR elements using Nastran© and the IDS *Bulkhead Sort* tool. *"Linear Static Analysis Method 2"*
3) Linear static analysis using Patran© with "ShearShells" elements. *"Linear Static Analysis Method 4"*.
4) Linear static analysis using Patran© with modified stiffness properties. *"Linear Static Analysis Method 5"*.
5) Linear static analysis using an ABAQUS model converted to Nastran©. *"Linear Static Analysis Method 6"*. Same results as *"Linear Static Analysis Method 2"*.
6) Nonlinear static analysis with fully effective quad elements using the Patran© *Results, Create, Free Body* tool. *"Non-Linear Static Analysis Method 1"*.
7) Nonlinear static analysis using Patran© and fully effective quads to analyze the model and use ABAQUS Viewer for post processing. *"Non-Linear Static Analysis Method 3."*
8) Nonlinear static analysis with fully effective quad elements using ABAQUS© Viewer and extracting the section forces. *"Non-Linear Static Analysis Method 7"*

Of these 8 methods investigated only two will be compared and they are the 2nd and the 6th method. The 2nd method is the traditional linear static analysis method using NASTRAN© CSHEAR elements and the 6th method is the proposed nonlinear static analysis using fully effective quad elements and ABAQUS© as the solver.

The resulting load distribution in the chords, stiffeners web for the linear static analysis and the nonlinear static analysis is shown in Figure 15 and Figure 16 respectively. The one

notable difference is the presence of extensional forces in the web (fx and fy), which are not accounted for in CSHEAR elements in the linear static analysis.

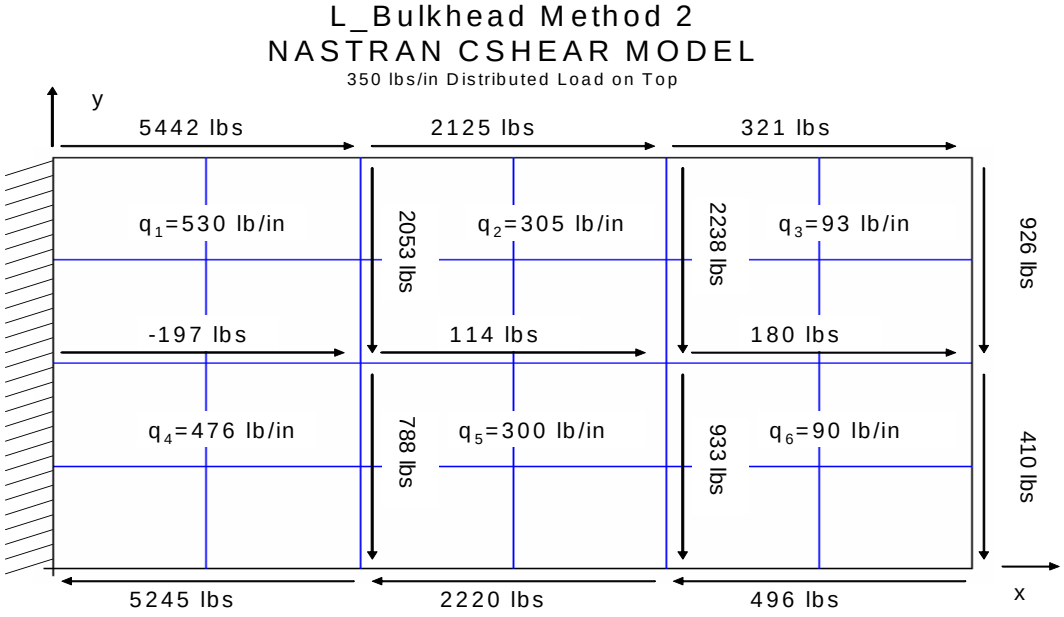

Figure 15 - Load distribution for linear static analysis with CSHEAR elements.

The linear static analysis results in Figure 15 shows from the analysis, that there is less load passing through the webs and therefore more load redistributed to the chords and stiffeners when compared to the nonlinear static analysis in Figure 16. Here in Figure 16, the webs are carrying more load and therefore less load is present in the stiffeners and chords.

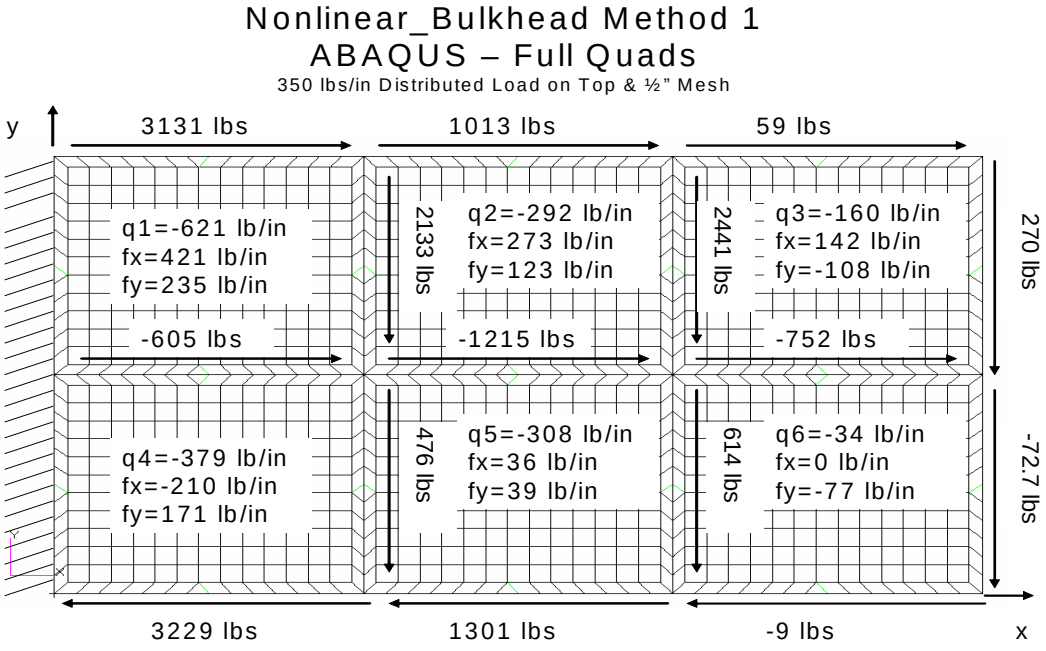

Figure 16 - Load distribution for nonlinear static analysis with ½" mesh.

A strain energy comparison was performed on these two models and the linear static analysis using CSHEAR elements contains more strain energy and therefore is more compliant.

To validate the load distribution of the two analysis models a free body cut at specified intervals was made in order to compare the shear and moment through the cantilever bulkhead. Figure shows the values of the moment in the bulkhead for the linear static analysis, the nonlinear static analysis and the theoretical hand-calculation. Various mesh densities were also investigated in the nonlinear static analysis, however in keeping with the mesh convergence study previously performed, a ½" mesh will be the main focus for the nonlinear static analysis. From Figure 17 it is clear that the moment distribution in the free-body cuts is nearly identical and therefore implies that the two analysis types are indeed comparable and loaded correctly.

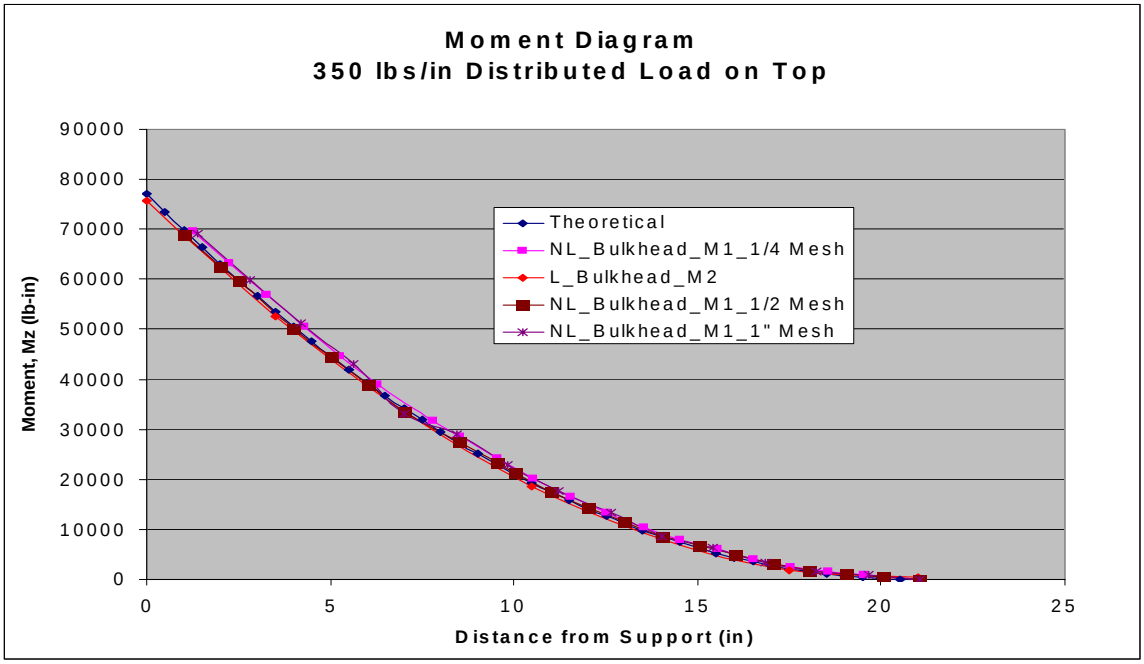

Figure 17- Free body cut of bulkhead moment.

Now that the analyses have been performed and the load distributions validated, the parts, which include the chords, stiffeners, and webs are sized for the load magnitudes for stress and buckling using analytical stress calculations. One bulkhead was however designed using FEA results and von Mises failure criterion alone with a ¼" mesh and compared with the analytical results of the ½" and 1" mesh. Another point to add was the bulkhead was sized for a margin of safety of 10% over any critical failure criterion and comparing the weight. This is in contrast to sizing all the parts the same and comparing the margin of safeties. The results are questionable from a manufacturing standpoint considering that some webs will be sized differently than others and the thickness tolerances will be under the minimum tooling allowable, in some cases, but these issues will be relaxed for this study in order to report a weight savings in the comparison. Furthermore ignoring the manufacturing tolerances and designing for the stress and buckling criterion the part is neither under nor over-designed.

Analysis Method	Total Volume: (in^3)	Total Weight (lb)	Weight Savings (%)
Linear-Bulkhead Method 2 - with CSHEAR elements	24.90829	2.540645	0
NL-Bulkhead Method 1 with 1" Mesh	22.56123	2.301246	9.422795
NL-Bulkhed Method 1 with 1/2" Mesh	23.77301	2.424847	4.775486
NL-Bulkhead Method 1 with 1/4" Mesh Designed with FEA alone	21.76126	2.219649	12.63446

Figure 18 - Bulkhead design comparisons for linear and nonlinear analyses

It is apparent from Figure 18 that the bulkhead that was analyzed and designed is in general on the smaller side with a low overall volume and weight. However, it is a representative model of an actual airframe bulkhead and the means and methods in designing the part is likewise representative of a true design. It is not the intent to extrapolate these results towards the application of a large scale bulkhead, but rather to investigate the advantages/disadvantages of using a nonlinear analysis versus a linear analysis and furthermore the effects of the mesh density on the design. From Figure 18 is shown that there will be a general weight savings in using a nonlinear static analysis with a ½" from that using a linear static analysis using CSHEAR elements. A couple of more items to note are that the webs are designed in the nonlinear analyses methods using both the shear flow and extensional forces (fx and fy). The overall design of the bulkhead with the ¼" mesh using FEA and von Mises criterion inherently accounts for buckling and the diagonal tension factors and therefore is designed without additional assumptions and modifications.

4. Cost Savings and Benefits

This new process of performing high resolution non-linear finite element analysis for sizing of parts earlier in the design phase for all parts will lead to cost savings in many ways. The cost savings are all based upon improving our ability to accurately predict load paths.

The first form of savings is to be able to predict failures in a design that otherwise would have gone undetected until entering test. It has been seen from past experience that each time a design flaw is detected before entering test; the cost would be avoided of having to re-design and re-test the part. This is usually on the order of a few hundred thousand dollars for each defect caught.

Another form of cost savings, or avoidance, is decreasing testing requirements. As budgets become tighter, there is a desire to reduce cost in any way it can be without compromising the quality of the products. One of the most expensive parts of producing new products is the testing phase. Much testing that is performed is done for the purpose of determining structural behavior, not material. As our own, and our customers' confidence in these improved analytical methods increases, there could be a reduction in the amount of testing for determining structural behavior. This level of cost reduction can be quite significant for a new program, particularly when you look at the cost of performing full aircraft testing.

Another form of cost savings to be mentioned is the possibility that more accurate analysis will lead to a more efficient design, and thus lead to weight savings. It was found during this year's research project that the parts, when sized to the non-linear results were showing around a 10%

decrease in weight. In the aircraft industry, a reduction in weight is a huge benefit, because any weight taken out of the structure is more payload capacity.

5. Conclusions

1. As can be seen from the stiffness differences between the non-linear modeling methods and the CSHEAR based loads modeling methods it is difficult to assess the effects of the assumptions made by the CSHEARs on the load distributions. It would seem clear, though that whatever distribution obtained by such methods would not nearly be as accurate as that obtained by a non-linear, post-buckled analysis. It is also not certain that the use of CSHEAR elements for thin parts would consistently produce conservative results for the airframe.
2. There are a number of key questions, which must be answered before fully implementing non-linear detailed FEA for both internal loads modeling as well as for detailed stress analysis. These questions and a short answer are summarized below.

    a. What mesh density would be required to adequately capture the post-buckled internal loads distribution? Mesh convergence studies seem to point to a minimum of 12 elements across the minimum dimension of the bay. For current Boeing rotorcraft, with 6" bays typically, this leads to a ½" mesh density. Even at ½" there is still some fluctuation in the results, and so 24 elements or more across the bay (or ¼" mesh in this case) would be most desirable, but the computing cost would be high at that mesh density.
    b. For a long web bay, can the aspect ratio of the elements be higher than 1:1, to save DOF in the model? There seems to be some tolerance to this from the convergence studies.
    c. What modeling/solution approach could be taken to obtain a converged solution reliably for many load cases? It is apparent that all the models must be run with non-linear geometry, using inertia relief to balance the rotor hub loads. In order to obtain a converged solution, it was necessary to use damping. It was found that creating dashpots in DOF 1-3 at each node in the model lead to a consistently converged solution. Although runtime can be decreased with higher damping coefficients, care must be taken not to affect the solution. A damping coefficient of .02 for the dashpots seemed to work well. The use of initial imperfections can have similar effects on runtime with the same hazard of affecting the results, but the increase in total runtime due to having to extract eigenvalue based results (normal modes or buckling modes), was too expensive to give benefit. There are many modes for such a complex full aircraft model as used here. It was decided to forego the initial imperfections due to runtime considerations. Although this has the hazard of failing to initiate a buckle, or to not obtain the correct post-buckled response, it is considered to be a low risk due to the fact that no aircraft geometry is perfectly planar or loaded perfectly planar.
    d. What are the effects on load distribution and part sizing from using post-buckled loads models? As can be expected, parts of the aircraft which formerly were idealized to carry only shear load, such as webs and skin panels, now carry

considerable extensional loads. This naturally reduces the load in chords and longitudinal members. The overall effect is to shift material away from the chords and into webs, but this results in a net decrease in material. In the study performed, there was approximately a 10% decrease in total weight of the part over the CSHEAR based model.

6. Acknowledgements

Although there are many people who have made it possible to move this technology forward, special thanks goes to Dr. Pierre Minguet for his technical guidance over the years.

7. References

1) ABAQUS User's Manual
2) PATRAN User's Manual
3) NASTRAN User's Manual
4) Gere, James M. and Timoshenko, Stephen P. (1997). Mechanics of Materials, Fourth Edition. PWS publishing company.
5) Ragab, Abdel-Rahman and Bayoumi, Salah Eldin (1999). Engineering Solid Mechanics, Fundamentals and Applications. CRC Press.
6) Boeing Company (1994). Boeing Design Manual, Volumes I and III. The Boeing Company, Seattle, WA.